ARCHIVES OF MECHANICS
Arch. Mech. **72** (4), 323–353, 2020, DOI: 10.24423/aom.3536

Non-linear modelling of elastic hysteretic damping in the time domain

C. SPITAS[1)], M. M. S. DWAIKAT[2)], V. SPITAS[3)]

[1)] *Nazarbayev University, Kazakhstan, e-mail: cspitas@gmail.com*

[2)] *An-Najah National University, Nablus, Palestine, e-mail: m.m.dwaikat@najah.edu (corresponding author)*

[3)] *National Technical University of Athens, Greece*

Elastic hysteretic damping is defined as the dissipation of energy at a rate that is weakly dependent on frequency of vibration. In this article, we propose that the elastic hysteretic damping can be achieved by a simple modification to the viscous damping model. The proposed modification is based on computing an instantaneous correction factor that recursively depends on the state variables of the system. This correction factor is related to the rate by which the velocity changes with respect to the displacement. The new model compares quite favourably with the other existing solutions in the time-domain and differences between the solutions become evident for higher damping ratios. It is found that the new model predicts consistently the weak variation in the loss factor as a function of frequency. In addition to its simple mathematical formulation, the proposed model is superior to the existing solutions in that it does not require knowledge of the past history of motion neither the knowledge of the excitation frequency and is extensible to any type of loading. Various aspects pertaining to the linearity of the proposed approach are finally discussed.

Key words: hysteresis, damping, modified viscous model, dynamics time-domain, mechanical vibration, frequency, non-linear modelling.

1. Introduction

Damping, which is a measure of energy dissipation during vibration, is an essential component to the understanding of dynamic behaviour of any structural system and vital for the design of earthquake-resistant structures [1, 2]. Generally speaking, there are two types of damping: the first is the frequency-dependent damping, so called viscous damping, and the second is the frequency-independent damping, so called hysteretic damping. While the viscous damping is mathematically simple and easy to implement in dynamic analysis, it is the least accurate and does not represent the realistic behaviour of most of structural assemblies or materials. In viscous damping, the dissipated energy per cycle scales linearly as a function of the frequency of vibration. Generally, most materials and structures dissipate energy via hysteretic behaviour, i.e. with very

weak dependence on the magnitude of vibration frequency [3]. However, such behaviour is generally complex in terms of its mathematical models, sometimes requiring convolution integrals that are difficult to generalize into structures of multi-degrees-of-freedom.

Mechanisms for hysteretic energy dissipation include elastic hysteresis, which is associated with recoverable deformations and internal friction among other factors, and of plastic hysteresis, which is associated with yielding and other mechanisms that relate to non-recoverable deformations and internal damage of materials or components. In our paper we focus on elastic hysteresis with the assumption of constant stiffness and no damage mechanisms.

The elastic hysteretic damping idea was first postulated by Kimball and Lovell [4] based on their experimental observation. Their idea was that the viscous damping model has to be modified so that the resulting dissipated energy is independent of the frequency of motion. The change was introduced by Collar, as mentioned in Bishop and Neumark [5, 6], into the time-domain equation of motion by replacing the viscous damping coefficient by another one that is inversely proportional to the harmonic forcing frequency. This tempted others [7–11] to consider the equivalent frequency-domain equation of motion which then appeared to have a complex stiffness term. This led others to consider the complex-stiffness model as equivalent to the hysteretic model for all cases including the free vibration case [12, 7].

This kind of generalization caused a debate whether the structural hysteresis model, with its complex form, violates the causality principle or not. According to the work of Caughey and Crandall [9, 10, 13], the structural hysteresis model is non-causal, in a sense that when it is subjected to a Dirac-delta $\delta(t)$ type of impulse excitation at time $t = 0$, it generates response even for $t < 0$. This supposition caused many authors that followed to try to "correct" for this non-causality effect [14–17] Some authors manipulated Hilbert transforms to achieve causality [14, 18], or used convolution integrals of the past history of motion to achieve causal hysteretic damping [19–21]. However, other researchers, such as Scanlan [22], maintain that the non-causality is a result of the wrong application of the model out of its context and due to the assumption that the damping ratio is constant and real. Recently, Bobrovnitskii [23], has presented a rigorous mathematical proof that the complex stiffness model, contrary to common belief, does satisfy causality. The proof necessitates that the Dirac impulse load, and in fact any load, should be constructed such that at $t < 0$ it should not exist for it to qualify as a physical load. However, the same proof procedure showed that such a system is Lyapunov unstable.

This confusion on causality encouraged other researchers to develop more phenomenological hysteresis models. This family of models, called the Bouc-Wen group of models [24–26], rely on internal non-physical, "state", parameters

for damping and also mix the energy dissipation due to stiffness nonlinearities, including the plastic degradation, along with the elastic hysteretic energy dissipation. Such models require pre-calibration for the case where it is intended to be used, which, in effect, makes them a cumbersome and ad-hoc, but effective solution to the problem of hysteresis nonlinearity.

Other models, such as the quasi-hysteretic model [15, 27] are based on cumulative correction of the dissipated energy at each time step based on the entire previous history of motion. In form, they look similar to the models that rely on Hilbert transforms for causality. Such a model can be tedious for computations and maybe impossible to apply in systems of multiple-degrees of freedom.

Other models revert to relating hysteresis force to be a dissipative frictional force that is proportional to displacement but in phase with velocity, such as Reid's model [12]. These models produce discontinuity in the internal force. Others tried to correct for such discontinuity [27, 28] by trying to "smoothen" the damping force by inserting gradual jump in the stiffness for a smoother transition function, thus in turn resulting in complicated models.

As seen from the brief review aforementioned, it is favourable to have a realistic and simple model in the time-domain, akin to the viscous model, that produces the hysteretic behaviour without the need for "complex" stiffness approach, neither for the integral transforms, nor non-physical internal parameters.

In this paper, we propose a simple modification to the viscous damping model such that the resulting behaviour is hysteretic. We propose to achieve this by applying a correction to the viscous model. The correction factor is computed based on the system local state variables (velocity, and displacement) at each time-step. However, before presenting the proposed modification, it is necessary to understand the development of the structural hysteresis model in its realistic context, then the various solutions by many researchers are presented whereby comparison of the models ensue.

2. The structural hysteresis model

The structural hysteresis model was initially proposed by KIMBALL and LOVELL [4], KUSSNER [29, 30] and further developed by KASSNER [31] for the study of fluttering effect in wings of planes. BISHOP and NEUMARK [5, 6] presented a realistic, and in our opinion essential, derivation of the structural hysteresis damping model starting with the viscous model. This derivation is essential since it puts the hysteresis model in its real context and facilitates its understanding. This is summarized below from [5] and [6] for the sake of completeness and to understand the realistic meaning of the complex stiffness hysteretic model.

Take the equation of motion for a single degree of freedom (SDOF) model with viscous damping:

$$kx + c\dot{x} + m\ddot{x} = F \tag{2.1}$$

where c is the viscous damping coefficient, k is the structural stiffness and m is its mass. The term $F_S = kx$ corresponds to the spring restoring force and the term $F_D = c\dot{x}$ to the damping force. When the excitation force is $F = F_0 \sin(\omega t)$, the steady state solution has the form $x^{(1)} = x_0 \sin(\omega t + \theta)$, and when $F = F_0 \cos(\omega t)$, the steady state solution has the form $x^{(2)} = x_0 \cos(\omega t + \theta)$. Evidently the two solutions are at a phase difference of $\pi/2$. If the excitation force is the vectorial sum $F_0[\cos(\omega t) + i \sin(\omega t)] = F_0 \mathrm{e}^{i\omega t}$, where $i = \sqrt{-1}$ is the imaginary unit, then the steady-state solution is simply the superposition (which is true for constant coefficients of Eq. (2.1)) $x = x^{(1)} + x^{(2)} = x_0 \mathrm{e}^{i(\omega t + \theta)}$. Now substituting the derivative for $\dot{x} = i\omega x$ in the equation of motion gives:

$$kx\left[1 + \frac{i\omega c}{k}\right] + m\ddot{x} = F = F_0 \mathrm{e}^{i\omega t}. \tag{2.2}$$

Since this equation is merely identical to the original viscously damped system above (Eq. (2.1)), the dissipated energy per cycle in Eq. (2.2) is equal to $\oint F_D \, \mathrm{d}x$, thus:

$$E = \oint c\dot{x} \, \mathrm{d}x = \pi \omega c x_0^2. \tag{2.3}$$

This dissipated energy is proportional to the driving frequency. To enforce the condition that the dissipated energy is independent of frequency, the fundamental assumption that $\omega c = gk$ is made, with g being the loss factor. Upon substitution into Eq. (2. 2) gives the conventional form of the complex stiffness damping model $F_S + F_D = kx(1 + \mathrm{i}g)$,where the loss factor g is seen to represent the ratio of the "complex" to the "real" stiffnesses. The dissipated energy per cycle in the hysteretic model can then be written as:

$$E = \oint ikxg \, \mathrm{d}x = \pi k g x_0^2. \tag{2.4}$$

The assumption $\omega c = gk$ is then used to define a "modified version" of a viscous damping that is hysteretic in its manifest behaviour, i.e.:

$$kx + \frac{gk}{\omega}\dot{x} + m\ddot{x} = F. \tag{2.5}$$

With $F_D = \frac{gk}{\omega}\dot{x}$ in this case. Note that this definition of hysteretic damping was essentially established based on a steady-state solution of a forced vibration with constant energy dissipation rate per cycle and constant driving fre-

quency ω. However, allured by its ability to render the viscously dissipated energy frequency-independent, the assumption $\omega c = gk$ is still used by a plethora of researchers [32, 10, 12] for free vibrations through its "corrected" version with the term $kx(1+ig)$ being used as the structural hysteresis model standing on its own. As previously discussed in the introduction, this caused a confusion later on about the meaning of the imaginary number in the time domain in an equation that is supposedly meant to describe real behaviour [33, 34]. On the other hand, certainly, the use of the original "viscous" model for cases of free vibration (i.e. Eq. (2.5) with $F = 0$) poses severe ambiguity regarding the value of ω.

In the next section, several solutions to the original corrected viscous and hysteretic models are mentioned in particular the free vibration case, and the differences and confusions between them are highlighted. Then we propose an alternate view on this issue by relating to the essence of how the hysteretic model has emerged in the first place.

2.1. Collar's solution as described by Neumark and Bishop

According to NEUMARK and BISHOP [5, 6], the solution to Eq. (2.5) with a harmonic excitation $F = F_0 \cos(\omega t + \theta)$ is straightforward and similar to that of Eq. (2.1). In a manner similar to the superposition of solutions as described earlier above, the steady-state solution for the forced vibration is assumed to have the form $x = x_0 \cos(\omega t + \theta)$, where by imposing the solution on Eq. (2.1) and using $\omega c = gk$, we have:

$$x_0 = \frac{\frac{F_0}{k}}{\sqrt{(1-(\omega/\omega_n)^2)^2 + g^2}} \cos(\omega t + \theta) \quad \text{and} \quad \tan(\theta) = \frac{g}{1-(\omega/\omega_n)^2}. \tag{2.6}$$

Similarly, for the case of free vibration, the transient solution is assumed to be a decaying function similar to that of viscously damped motion: $x = x_{0,f} \mathrm{e}^{-at} \cos(\omega^{(\mathrm{Col})} t + \theta)$. This solution is imposed on Eq. (2.5), and then the assumption $\omega^{(\mathrm{Col})} c = gk$ is utilized again. This gives

$$\begin{gathered} a = \omega_n \sqrt{\frac{1-\sqrt{1-g^2}}{2}} \quad \text{and} \quad \omega^{(\mathrm{Col})} = \omega_n \sqrt{\frac{1+\sqrt{1-g^2}}{2}}, \\ x_{0,f} = \frac{x_0}{\cos(\theta)} \quad \text{and} \quad \tan(\theta) = \frac{v_0 + a x_0}{-\omega x_0}. \end{gathered} \tag{2.7}$$

Where x_0 and v_0 are the initial displacement and velocity, respectively. As it is clearly seen, this solution predicts a decrease in the damped natural frequency, which is confirmed by experiments. However, this reduction is constant all over the entirety of motion, which is something not yet confirmed by experimentation. On the contrary, some experiments on the free vibration of small metal cantilever

beams provide evidence that neither the frequency of motion nor the damping ratio is constant all over the motion [35, 36].

This solution assumes linearity of the equation of motion which necessitates the damping coefficient (gk/ω) to be a constant throughout the motion.

2.2. Solution by Neumark for free vibration

Neumark [6] agrees with the previous solution for the case of forced vibration. However, in the case of free vibration, there is an ambiguity in defining the frequency term in the Eq. (2.5). Also, the validity of the assumption $\omega c = gk$ is questioned since the dissipated energy in the viscously damped system for free vibration can no longer be measured by Eq. (2.3). Neumark proposed a solution to this problem based on a "mean energy" concept. In his approach, he imposed the criteria that the lost energy be frequency-invariant by equating the mean value of the dissipated energy per cycle in a decaying motion to that of an equivalent viscously dissipated energy.

Assuming the free decaying vibration motion resulting from Eq. (2.5) is described as $x = x_0 \mathrm{e}^{-at}\sin(\omega t + \theta)$, the dissipated energy per cycle in a viscously damped system becomes:

$$E = \oint c\dot{x}\mathrm{d}x = \frac{1}{4}cx_0^2(1 - \mathrm{e}^{-4\pi a/\omega})\left(\frac{\omega^2}{a} - \omega\sin(2\theta) + 2a\sin^2(\theta)\right). \tag{2.8}$$

Of which the mean dissipated energy per cycle is

$$E_m = (\pi c\omega x_0^2)\frac{(1 - \mathrm{e}^{-4\pi a/\omega})}{4\pi a/\omega}\left(1 + \frac{a^2}{\omega^2}\right). \tag{2.9}$$

Now the fundamental assumption taken by Neumark is to equate this mean value of dissipated energy to the dissipated energy of the hysteretic model on the mean value:

$$E_m = \pi k g x_m^2. \tag{2.10}$$

Thus requiring that $c\omega = kgN$ where N is a coefficient resulting from equating Eq. (2.9) to Eq. (2.10); x_m^2 is the square of the mean value of the response, and is taken to be equal to the arithmetic average of the squares of the amplitudes at the beginning and end of a cycle.

The solution by Neumark captures in an analytical form the hysteretic damped frequency of the free vibration as:

$$
\begin{aligned}
\omega^{(\mathrm{Neu})} &= \frac{4\pi\omega_n}{\sqrt{16\pi^2 + [\ln((1+\pi g)/(1-\pi g))]^2}},\\
a &= \frac{\ln((1+\pi g)/(1-\pi g))}{\sqrt{16\pi^2 + [\ln((1+\pi g)/(1-\pi g))]^2}},\\
N &= \frac{(8\pi/g)\ln((1+\pi g)/(1-\pi g))}{16\pi^2 + [\ln((1+\pi g)/(1-\pi g))]^2}.
\end{aligned}
\tag{2.11}
$$

This solution is only valid for $g < 1/\pi$ and as seen, it also predicts constant value for the damped frequency over the entirety of motion. Further, this solution produces a decrease in the natural frequency due to damping which conforms to experimental observations, which puts it in the same trend like the previous solution.

2.3. Solution by Chen *et al.*

In this solution CHEN *et al.* [37] realize that the frequency of the response under free vibration may not remain constant throughout the motion. Rather, they postulate that it alternates between two values depending on its state (i.e., the combination of response and its derivative). This is justified by the authors [37] through saying that the damping force must be in-phase with the velocity. When the response x and its derivative $\dot{x}$ are in the first or the third quadrants of the phase plane, i.e. $x\dot{x} > 0$ then $\omega = \omega_n\sqrt{1+g}$, and if they are in the second or fourth quadrant, i.e. $x\dot{x} < 0$ then $\omega = \omega_n\sqrt{1-g}$. Using this understanding, the authors combined the "traveling time" for the four quadrants and used it to compute an overall "effective" natural frequency ω_{Ch} for a complete cycle. This effective natural frequency is nothing more than a sort of averaging of the two limits of the damped frequency. Later on, the authors assumed this "effective" natural frequency to remain constant throughout the motion.

By this approach, the solution for the free vibration of hysteretic damping is:

$$
\begin{aligned}
x &= Z\left[x_0\cos(\omega^{(\mathrm{Ch})}t) + \frac{v_0}{\omega}\sin(\omega^{(\mathrm{Ch})}t)\right],\\
\omega^{(\mathrm{Ch})} &= 2\omega_n\left(\frac{\sqrt{1-g^2}}{\sqrt{1-g}+\sqrt{1+g}}\right),\\
Z &= \left(\frac{1-g}{1+g}\right)^{\frac{\omega t}{2\pi}}.
\end{aligned}
\tag{2.12}
$$

Similar to the previous solutions, this one generally predicts slightly more significant reduction in the damped natural frequency and it tends to overestimate the response values when compared to all other solutions. The interesting

thing about this solution is that it postulates that the damped frequency itself may oscillate between two limits depending on reversal of motion or reversal of speed direction. However, they maintain that the damping ratio remains constant throughout the motion. It is worth mentioning that due to the lack of high quality testing on this kind of behaviour, it is impossible to judge such a postulate.

2.4. Solution by Ribeiro *et al.*

Ribeiro *et al.* [16, 38, 39] proposed to look at Eq. (2.2) from a purely mathematical perspective. Ribeiro *et al.* speculated that the solution must be complex by necessity and the physical response of the system should be the real part of $x(t)$. As shown in Ribeiro *et al.* [16], the solution is given by (after discarding the unstable part of the solution):

$$x(t) = \mathrm{C}\mathrm{e}^{-\omega_n a t}\mathrm{e}^{\omega_n b t} \tag{2.13}$$

where C is a complex constant and a and b are given as:

$$a = \sqrt{\frac{-1+\sqrt{1+g^2}}{2}} \quad \text{and} \quad \mathrm{b} = \sqrt{\frac{1+\sqrt{1+\mathrm{g}^2}}{2}}. \tag{2.14}$$

The solution is done by imposing imaginary as well as real initial conditions, which upon discarding the imaginary solution, the real "observable" solution is:

$$x(t) = \mathrm{e}^{-\omega_n a t}\left(x_0\cos(\omega_n b t) + \frac{v_0+\omega_n a x_0}{\omega_n b}\sin(\omega_n b t)\right). \tag{2.15}$$

This solution produces a damped frequency of the hysteretic response slightly larger than the viscously damped frequency. Also it results in a storage modulus that increases with frequency.

Maia [33] investigated the validity Ribeiro et al. solution in terms of causality when subjected to a Dirac impulse, and came to a conclusion that the solution is inconsistent in a sense that it does not solve the initial problem, but rather only the real part of it. Maia tried to provide a remedy to this inconsistency.

It is clear from the previous studies that the habit of discarding "imaginary" items simply because they are non-real, causes further confusion in the interpretation of the results when using the complex-stiffness model for hysteresis. Also, all these solutions require prior knowledge of either an external forcing frequency, or the eigenfrequency of the SDOF system, making them cumbersome and impractical to apply in practice.

Furthermore, these models assume constant damping through the entire motion, which is a necessity in order to use superposition principles and frequency-domain techniques for solving the equation of motion. This supposition is found

inconsistent with experiments [36] and may lead to inconsistent consequences, mainly the non-causality issue [12] when transferring the equation of motion to the frequency-domain. Therefore, it is wise to develop another understanding of the hysteresis phenomenon away from the use of complex numbers, and does not necessitate the constancy of the damping term gk/ω.

3. Proposed solution

In this approach, a constitutive model is developed on the basis of the instantaneous state of a SDOF vibrating system, which is applicable regardless of whether a vibration is forced or free, or harmonic, periodic or otherwise, and without prior knowledge of the external excitation and its parameters[1].

Going back to the origins of the hysteresis damping model as engineered by KUSSNER [29, 30] and KASSNER [31], the value of ω in the equation of motion of Eqs. (2.2) and (2.5) is a result of a steady-state solution of a forced vibration. Also, inspired by the idea that the natural frequency in the hysteretic model need not remain constant, as shown by CHEN *et al.* [37], and the need to arrive at a frequency-independent hysteretic behaviour a new model is proposed for hysteresis damping based on a simple modification to the viscous damping model.

In the viscous model, the dissipated energy per cycle scales up with the amount of the driving frequency. This indicates that for the dissipated energy per cycle to remain constant, there should exist an internal mechanism that works in opposite effect to the driving frequency. This is equivalent to defining the viscous damping property to be inversely proportional to the driving frequency, i.e. the same assumption taken by Collar, Bishop and Neumark (i.e. $\omega c = gk$). At the same time, we note that in case of free vibration there is no such external "driving" frequency. Also, even in the context of a forced vibration other than a simple harmonic excitation, a single constant driving frequency may not be defined.

Instead, since the viscous damping force depends on the velocity, it is conceivable to think of the hysteretic damping as somehow inversely proportional to the rate at which the velocity changes with respect to the displacement re-

[1]Even though the model describes instantaneous states, the entire concept of hysteretic damping and of related metrics such as the loss factor g is defined on the concepts of "oscillation" and "energy lost per cycle", so at times references will be made to magnitudes such as "amplitude", (pseudo)"frequency" and "loss factor", even though none of these are defined outside of periodic motion. As we explain in the model, we make use of an approximation of the instantaneous state of the system by a harmonic oscillation and in that context "amplitude", "frequency" and "loss factor" may be used validly and without loss of the generality of the model. This also helps to maintain compatibility with the terminology established in the literature. The reader is cautioned to avoid any confusion that might arise from such use of terminology and is redirected to Sections 1–2, where the matter has been discussed at length.

sponse, i.e.: $\frac{\mathrm{d}v(t)}{\mathrm{d}t}/x(t)$. Therefore, let the instantaneous response $x(t)$ within the time interval $[t, t+\delta t]$ be a part of an elementary harmonic oscillation, i.e. we approximate $x(t)$ within a small vicinity of t as a harmonic oscillation:

$$x(t) = \tilde{x}_{\mathrm{ins}} \sin(\omega_{\mathrm{ins}} t + \theta_{\mathrm{ins}}), \qquad t \in [t, t+\delta t] \tag{3.1}$$

where ω_{ins} is the frequency of this approximate harmonic oscillation and will thereafter be called "instantaneous correction factor", or "instantaneous pseudo-frequency" of the response. "Instantaneous" denotes the transient nature of this approximation and "pseudo" the fact that, in principle, the factor ω_{ins} does not represent a real frequency of the response[2], per se, and hence may not readily admit a physical meaning. At the same time, it is interesting to note that, if the response is purely harmonic (as e.g. in a steady-state solution to a harmonic excitation), this factor will be physically identical to the frequency of the response. Using Eq. (3.1), we can calculate:

$$\frac{\text{rate of change of velocity}}{\text{displacement}} = \frac{\frac{d}{dt}v(t)}{x(t)} = \frac{\frac{\mathrm{d}^2}{\mathrm{d}t^2}x(t)}{x(t)} = -\omega_{\mathrm{ins}}^2. \tag{3.2}$$

The instantaneous pseudo frequency defined in Eq. (3.2) is used as a correction factor to the viscous damping model. This factor is computed from the real response at each time step using the definition in Eq. (3.2) using the immediately prior (known) state, i.e. the displacement response and its backward time differences. The damping force of the thus "corrected" viscous damping model (Eq. (2.5)) can then be written as:

$$F_D = g\frac{k}{\omega_{\mathrm{ins}}}\dot{x}. \tag{3.3}$$

The coefficient g, which can be readily understood to correspond to the loss factor, can be determined by imposing that the viscously dissipated energy per cycle (if an entire cycle were allowed to complete) is constant:

$$E = \oint F_D \,\mathrm{d}x = \int_0^{2\pi/\omega_{\mathrm{ins}}} F_D \,\mathrm{d}x = \pi k g \tilde{x}_{\mathrm{ins}}^2 = 2\pi g \frac{1}{2} k \tilde{x}_{\mathrm{ins}}^2. \tag{3.4}$$

The value of $\frac{1}{2}k\tilde{x}_{\mathrm{ins}}^2$ represents the maximum restoring "elastic" energy in the system at that cycle. From Eq. (3.4) we get the known expression for the loss factor [40]:

$$g = \frac{E}{2\pi \frac{1}{2} k \tilde{x}_{\mathrm{ins}}^2}. \tag{3.5}$$

[2]In fact, there is no requirement that the response being approximated must be harmonic or even periodic.

Notice that this approach produces a pure frequency-independent hysteresis behaviour if the entire response is purely harmonic, which would be the result from a steady-state forced vibration under harmonic loading. In such a case, the calculated instantaneous pseudo frequency becomes equal to the forcing frequency. This solution bears resemblance in terms of the line of thinking to the solution proposed by NEUMARK [6]. In his solution, Neumark calculated the "corrected" frequency of motion by equating the energy loss per cycle of that of decaying hysteretic motion to that of decaying viscous motion. Thus, the Neumark solution is based on "integral" equivalence between viscous and hysteretic models. Our approach assumes the same line of thinking but instead of looking at the energy per cycle, we look at the "instantaneous" frequency of an equivalent harmonic response that makes the energy loss in the hysteretic motion invariant. Thus our approach is based on a somewhat "differential" equivalence between viscous and hysteretic damping. We insist on assuming the instantaneous motion to be equivalent to a harmonic because this is the original basis on which the whole hysteretic model was crafted by Kussner and used later on by Neumark and Bishop. Also, this is consistent with experimental observation that the loss factor remains nearly constant under varying harmonic excitation as demonstrated by KIMBALL and LOVELL [4] and others later on.

4. Recurrence solution and convergence

The proposed approach assumes continuous updating of the viscous factor $g\frac{k}{\omega_{\text{ins}}}$ in the damping force by a correction factor $\frac{1}{\omega_{\text{ins}}}$ using a differential estimator that depends on the local solution at that instant. This leads to a nonlinear recursive dependency between $\frac{1}{\omega_{\text{ins}}}$ and the response $x(t)$. Therefore, an iterative scheme can be employed numerically as follows: at each time increment "t_i", the equation of motion is solved assuming a pseudo-viscous damping model with damping force as in Eq. (3.3) and assuming an initial value of $(g\frac{k}{\omega_{\text{ins}}})_i^1$, where the superscript 1 indicates iteration 1. This produces a response $x_i^1(t)$ (at increment t_i) which is then used to make a better estimate for the factor $(g\frac{k}{\omega_{\text{ins}}})_i^2$ using Eq. (3.2). The second iterative step is to recompute the response $x_i^2(t)$ using the already corrected pseudo-viscous damping $(g\frac{k}{\omega_{\text{ins}}})_i^2$, and so on until the value of $(g\frac{k}{\omega_{\text{ins}}})_i^j$ stabilizes after iteration j. This numerical procedure is shown in the flow chart in Fig. 1, which shows how the value of the factor $\omega_{\text{ins}}$is obtained by iteration with each time increment.

In case of forced vibration with purely harmonic excitation, the steady state solution approaches a harmonic motion, i.e.: $\lim_{t\to\infty} x(t) = C\sin(\omega_0 t+\phi)$, where C is a constant, and ω_0 is the driving frequency. By virtue of its definition, the correction factor ω_{ins} converges to the driving frequency of motion ω_0.

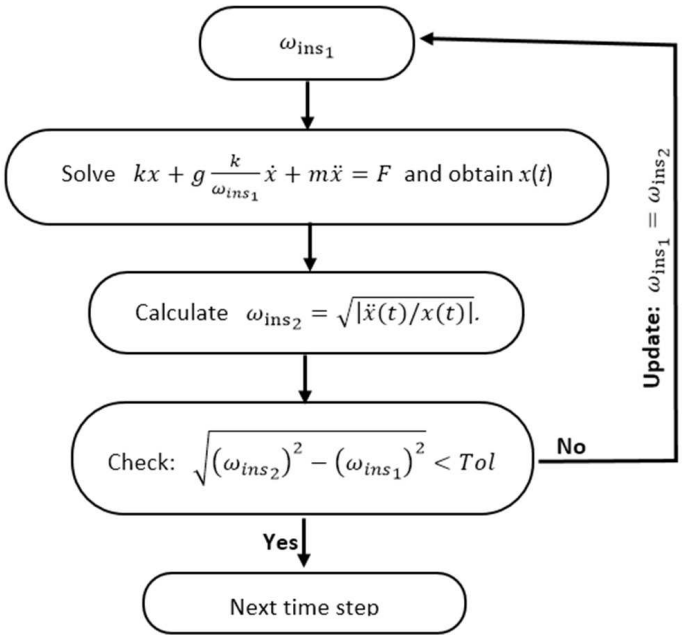

FIG. 1. A flow chart showing the proposed solution procedure within one-time increment.

In case of free vibration, we will have a look at what happens inside two consecutive iterations, j and $j+1$ for the same time increment "i". In effect, at increment t_i, we are solving the following equation of motion:

$$\omega_n^2 x + g\omega_n^2 \left[\frac{1}{\omega_{\text{ins}}}\right]_i^j \dot{x} + \ddot{x} = 0. \tag{4.1}$$

The generic solution at that increment can be expressed as:

$$x_i^j(t) = C \cdot \exp(\lambda_i^j (t - t_i))$$

where:

$$[\lambda_i^j]_{1,2} = -\frac{1}{2} g\omega_n^2 \left[\frac{1}{\omega_{\text{ins}}}\right]_i^j \mp \sqrt{\left(\frac{1}{2} g\omega_n^2 \left[\frac{1}{\omega_{\text{ins}}}\right]_i^j\right)^2 - \omega_n^2}. \tag{4.2}$$

Note that this solution is valid for the interval $t \in [t_i, t_i + dt]$ if we assume that ω_{ins} is constant in this interval. The general solution then is:

$$x_i^j(t) = C_1 \cdot \exp([\lambda_i^j]_1 (t - t_i)) + C_2 \cdot \exp([\lambda_i^j]_2 (t - t_i)) \tag{4.3}$$

where the constants C_1 and C_2 must be determined using the initial conditions for this increment, which are of course the values at the end of the previous time

increment. Thus at $t = t_i$, we have: $x = x_i$, and $\dot{x} = \dot{x}_i$. Solving for C_1 and C_2 gives:

$$C_1 = \frac{x_i[\lambda_i^j]_2 - \dot{x}_i}{[\lambda_i^j]_2 - [\lambda_i^j]_1} \quad \text{and} \quad C_2 = \frac{-x_i[\lambda_i^j]_1 + \dot{x}_i}{[\lambda_i^j]_2 - [\lambda_i^j]_1}. \tag{4.4}$$

Using the solution Eq. (4.3), the instantaneous local correction can be calculated as $\omega_{\text{ins}} = \sqrt{|\ddot{x}_i/x_i|}$, which, after algebraic simplification gives an improved estimate for ω_{ins}:

$$\begin{aligned} \omega_{\text{ins}}]_i^{j+1} &= \sqrt{\left|\frac{\dot{x}_i}{x_i}([\lambda_i^j]_1 + [\lambda_i^j]_2) - [\lambda_i^j]_1[\lambda_i^j]_2\right|} \\ &= \sqrt{\left|g\omega_n^2\left[\frac{1}{\omega_{\text{ins}}}\right]_i^j \frac{\dot{x}_i}{x_i} + \omega_n^2\right|}. \end{aligned} \tag{4.5}$$

Equation (4.5) is a nonlinear recurrence relationship that is impossible to solve for an iteration j. However, it can be shown that this recursive equation is convergent as $j \to \infty$ as long as $x_i \neq 0$.

In order to find the convergence limits for the recursive equation Eq. (4.5), we need to look for the candidate fixed points. To achieve this, assume that as $j \to \infty$, the value of $[\omega_{\text{ins}}]_i^j$ approaches the limit ω_{ins}:

$$\begin{aligned} \lim_{j\to\infty}[\omega_{\text{ins}}]_i^j &= \lim_{j\to\infty}\left(\sqrt{\left|g\omega_n^2\left[\frac{1}{\omega_{\text{ins}}}\right]_i^j \frac{\dot{x}_i}{x_i} + \omega_n^2\right|}\right) \\ &= \omega_{\text{ins}} = \sqrt{\left|\frac{g\omega_n^2}{\omega_{\text{ins}}}\,\frac{\dot{x}_i}{x_i} + \omega_n^2\right|}. \end{aligned} \tag{4.6}$$

The solution to Eq. (4.6) yields a characteristic cubic polynomial in ω_{ins}, which absolutely guarantees the existence of at least one real solution for ω_{ins}. Further, the solution depends on the signum of $\dot{x}_i/x_i$. In other words, it depends on the state of the system, as stipulated by CHEN *et al.* [37].

It can be easily seen that when $\frac{\dot{x}_i}{x_i} = 0$, the solution converges immediately to $\omega_{\text{ins}} = \omega_n$ with:

$$\omega_d = \omega_n\sqrt{1 - (g/2)^2}. \tag{4.7}$$

It is obvious too that the solution diverges numerically when $x_i = 0$. However, substituting $x_i = 0$ into Eq. (4.6) gives $\omega_{\text{ins}} = \infty$, which upon resubstitution back again and using L'Hopital's rule gives $\omega_{\text{ins}} = \omega_n$, thus the solution oscillates between $\omega_{\text{ins}} = \omega_n$ and ∞ for $x_i = 0$. When $\frac{\dot{x}_i}{x_i} \geq -\left(\frac{2}{\sqrt{27}}\,\frac{\omega_n}{g}\right)$, the recurrence

equation converges to the single real root of the characteristic polynomial generated from Eq. (4.6). For the case when $\frac{\dot{x}_i}{x_i} < -\left(\frac{2}{\sqrt{27}}\frac{\omega_n}{g}\right)$, the polynomial has 3 real roots, and the convergence is not warranted as it depends on the selection of the initial value for $[\omega_{\text{ins}}]_i^j$ and the sequence can behave chaotically. Generally, to guarantee convergence, the initial value should be selected near the real roots of the characteristic limit polynomial.

It is readily seen that we are solving a linear viscous equation per iteration, and if the time increment "Δt" is taken to be the period of one cycle of motion, then our approach comes in principle closer to that of Neumark, which equated the energy per cycle for both hysteretic and viscous models.

Notice that the recurrence solution (Eq. (4.5)) can be obtained directly using the equation of motion. By considering the Eq. (4.1), and re-arranging for $\ddot{x}_i/x_i$ and taking square root, then we immediately get to Eq. (4.5). This can also be done for the case of forced vibration under arbitrary force F_i (Eq. (1.1)) which then gives:

$$[\omega_{\text{ins}}]_i^{j+1} = \sqrt{\left|\frac{F_i/m}{x_i} - \omega_n^2 - g\omega_n^2\frac{\dot{x}_i}{x_i}\left[\frac{1}{\omega_{\text{ins}}}\right]_i^j\right|}. \tag{4.8}$$

Denoting $A = \frac{F_i/m}{x_i} - \omega_n^2$ and $B = g\omega_n^2\frac{\dot{x}_i}{x_i}$, the limit(s) ($\omega_{\text{ins}}$) for the sequence in Eq. (4.8) must satisfy the following cubic polynomial:

$$[\omega_{\text{ins}}]^3 - A[\omega_{\text{ins}}] - B = 0. \tag{4.9}$$

The convergence of Eq. (4.8) and existence of limits from the characteristic polynomial Eq. (4.9) depend on the signum of B (and hence, on the state ratio $\dot{x}_i/x_i$) and on the starting initial guess for ω_{ins}. One tool to explore convergence and limits of the recurrence relation is to qualitatively trace the sequence process on the graph of the generating function $F(\omega_{\text{ins}}) = \sqrt{|A + B/\omega_{\text{ins}}|}$ in Eq. (4.9), as shown in Figs. 2 and 3. In case $B > 0$ the generating function is strictly decreasing and bounded from below by the asymptote $F(\omega_{\text{ins}}) = \sqrt{|A|}$ as shown in Fig. 2a, and thus the sequence converges to the single real positive fixed point (single positive root for Eq. (4.9)).

However if $B < 0$, then the convergence depends on the starting initial guess for ω_{ins} as shown in Figs 2b and Fig. 3. This is due to the nature of the generating function for negative B. The sequence may behave chaotically as demonstrated in Fig. 2b where it may keep cycling around the fixed point with no convergence (Fig. 2b). However, a suitable choice of initial guess for ω_{ins} near the fixed point can lead to a definite convergence to either a single fixed point (Fig. 3a) or to multiple fixed points (Fig. 3b), depending on how many real positive roots exist for the polynomial in Eq. (4.9) and depending on the initial guesses (P_0, P_1

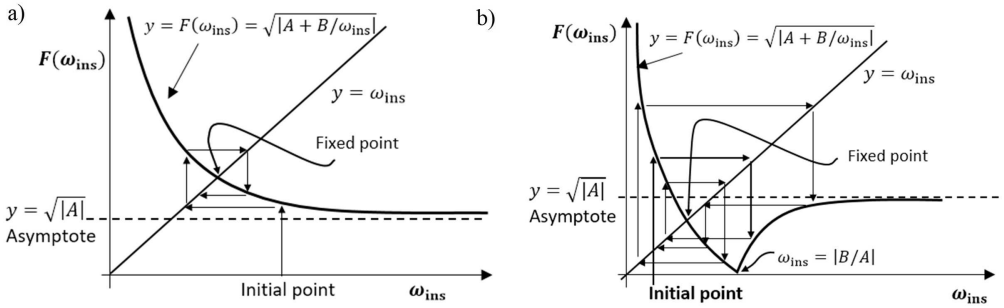

FIG. 2. Dependency of convergence of the Eq. (4.9) on the sign of $B = g\omega_n^2(\dot{x}_i/x_i)$, a) $B > 0$, and b) $B < 0$.

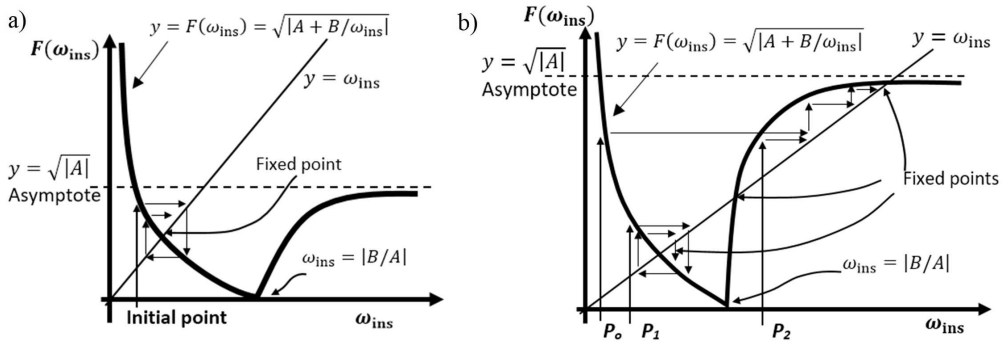

FIG. 3. Dependency of convergence of Eq. (4.9) on the initial guess: a) single real root and b) 3 real roots.

or P_2) for ω_{ins}. On either case, the convergence is always guaranteed if we take the initial guess very close to the fixed points. Given this, there is no need to carry out the iterations for convergence because we can simply jump straight to the real fixed points as solutions to the recurrence equation.

It should be mentioned here that the recurrence relation can also diverge (or oscillate) whenever the whole term under the square root in Eq. (4.8) becomes zero. This can simply be avoided by careful selection of the initial guess for ω_{ins} such that the term starts as non-zero under the square root.

Figure 4 shows the results of the converged local frequency ω_{ins} as computed for a free vibration case using the numerical iterative scheme and using the roots of the characteristic polynomial (Eq. (4.9)). Both techniques produce exactly identical results as expected. All points converged except the seemingly asymptotic spikes at all $x = 0$ points, which represent a numerical singularity as can be seen in Eq. (4.6).

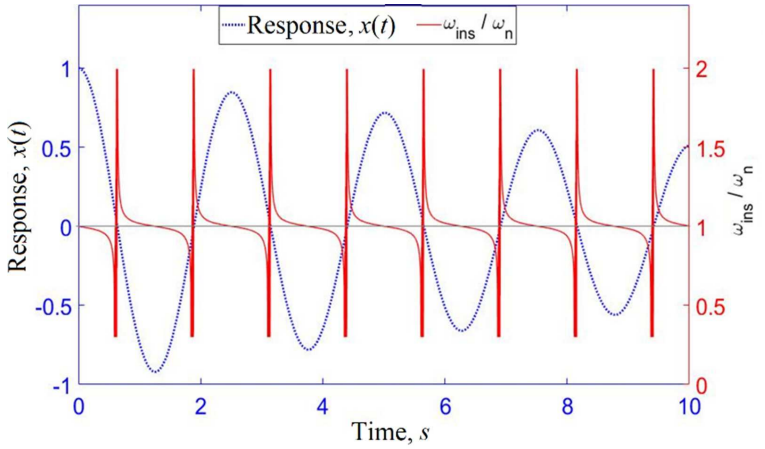

FIG. 4. The variation of the instantaneous correction factor ω_{ins} along the free response as obtained from the numerical iterative procedure and identically from the recurrence relation (Eq. (4.5)) ($g = 0.05$).

In the relatively brief simulation runs that were performed in the context of this work no numerical instabilities were observed – although it is conceivable that such will start to manifest, if the simulation continues for sufficiently long time.

Because the instantaneous correction factor is calculated based on the immediately prior states, the solution is always bound, in a sense, by said prior states. In addition, in a time-domain simulation the damping also tends to delay the onset of numerical-error-induced instabilities.

5. Comparative study

The proposed model is compared to the 4 solutions mentioned earlier for the case of free vibration of a SDOF. The four solutions presented earlier represent direct attempts to solve the original problem (Eq. (2.5)) in the time-domain. The new model is solved using central difference quotient (CDQ) method with a sufficiently small time increment $\Delta t \approx 10^{-3}\frac{2\pi}{\omega_n}$. The value of $\omega_{\text{ins}}$is calculated using an iterative procedure at each time increment until it stabilizes according to L2-norm tolerance of 10^{-3}:

$$\sqrt{(\omega_{\text{ins}}^2)^{j+1} - (\omega_{\text{ins}}^2)^{j}} < 10^{-3}. \tag{5.1}$$

The results for free vibration are presented in Figs. 5–8 for different damping ratios and natural frequencies. In these results, the proposed solution is conducted using two techniques, first is numerical via the direct CDQ iterative procedure

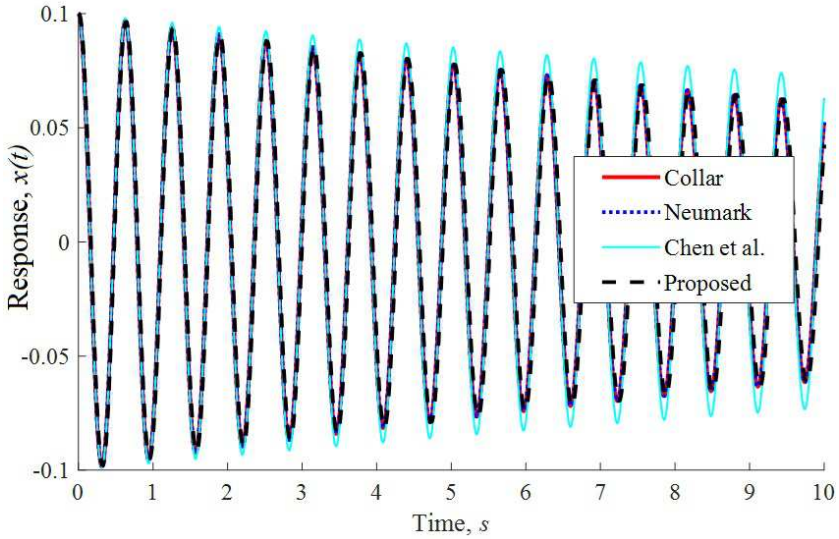

FIG. 5. Hysteretic free vibration response with loss factor $g = 0.01$ and $\omega_n = 10$.

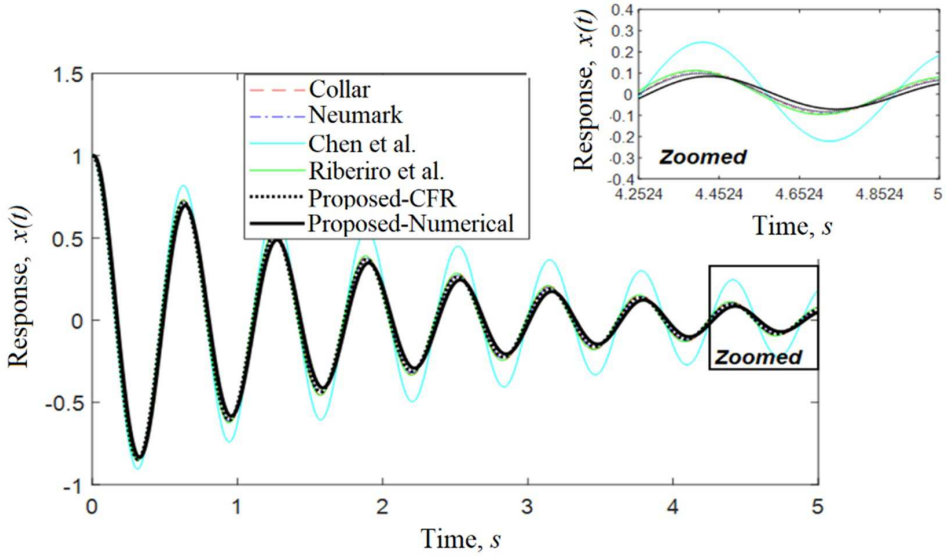

FIG. 6. Hysteretic free vibration response with loss factor $g = 0.1$ and $\omega_n = 10$. Proposed-CFR is the solution using the fixed points, Proposed-Numerical is the CDQ iterative solution.

as explained above, and the second (CFR) is using the fixed points from the cubic function (Eq. (4.9)), in case of multiple roots we resorted to the smallest root.

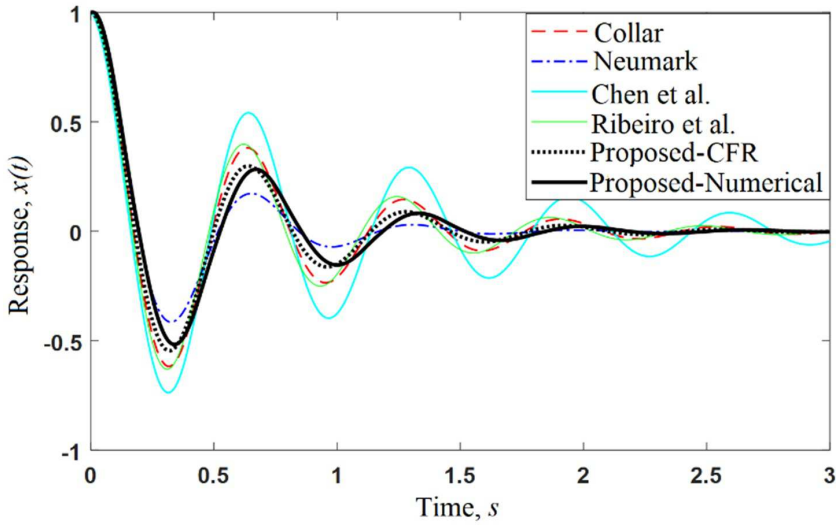

FIG. 7. Hysteretic free vibration response with loss factor $g = 0.3$ and $\omega_n = 10$. Proposed-CFR is the solution using fixed points, Proposed-Numerical is the CDQ iterative solution.

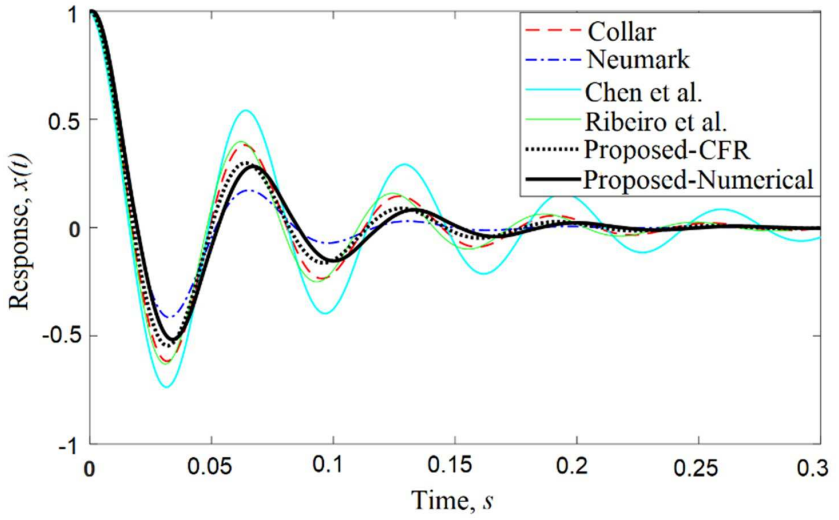

FIG. 8. Hysteretic free vibration response with loss factor $g = 0.3$ and $\omega_n = 100$. Proposed-CFR is the solution using fixed points, Proposed-Numerical is the CDQ iterative solution.

In the figures, the proposed method seems to go well with Collar and Neumark solutions for a small value of loss factor, and comes in between the two for higher values of loss factor. On the other hand, the solution by Chen *et al.*, which

assumes averaged value for the frequency, produces larger amplitudes compared to the others. The differences, albeit small, become more evident for higher values of loss factor. The solution by Ribeiro *et al.* seems to match well with Collar's solution, and this is expected since that solution assumed direct substitution of a complex response and then considered the real answer, which is not far from Collar's direct substitution method. Overall, the proposed method produces results that are pretty similar to the other methods, such as COLLAR [7], NEUMARK [6], CHEN [37] and RIBEIRO [38] although small differences in their predictions exist. At this time, however, there are no available sufficiently precise experimental data sets from ideal SDOF systems that could allow a final judgement as to which prediction is the most accurate. Moreover, while in reasonably good agreement with the rest, the proposed approach has the privilege of simplicity and generalisability over the other solutions for any kind of loading scenario, not only harmonic as is shown in Section 7.

In Figs. 9–11, we compare the proposed solution versus Collar's and the viscous solutions for the hysteresis loops in case forced and free vibration. The

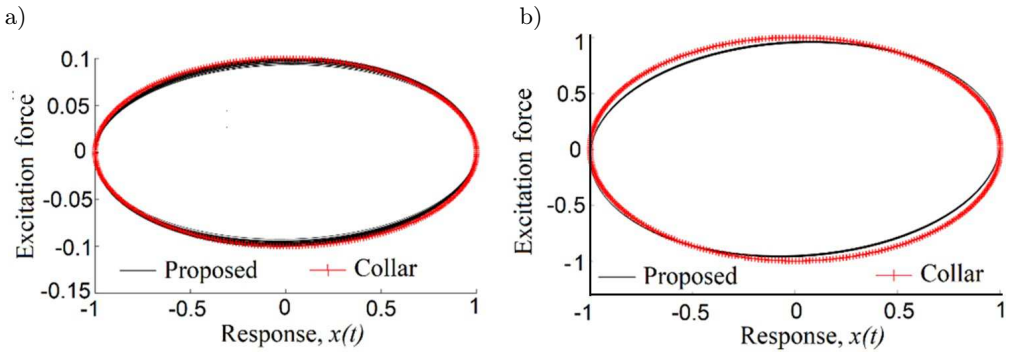

FIG. 9. Hysteresis loops at steady-state of harmonically forced vibration at resonance frequency, a) $g = 0.1$, b) $g = 0.01$.

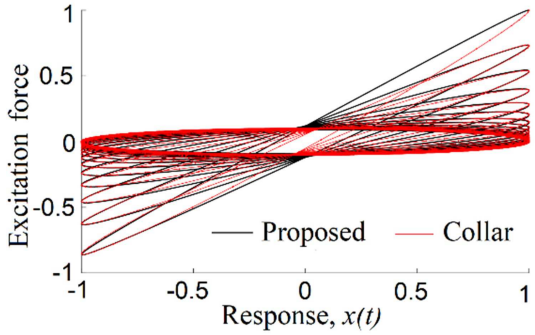

FIG. 10. Hysteresis loops at harmonically forced vibration at resonance frequency, including the transient phase, $\omega_n = 1$, $g = 0.1$.

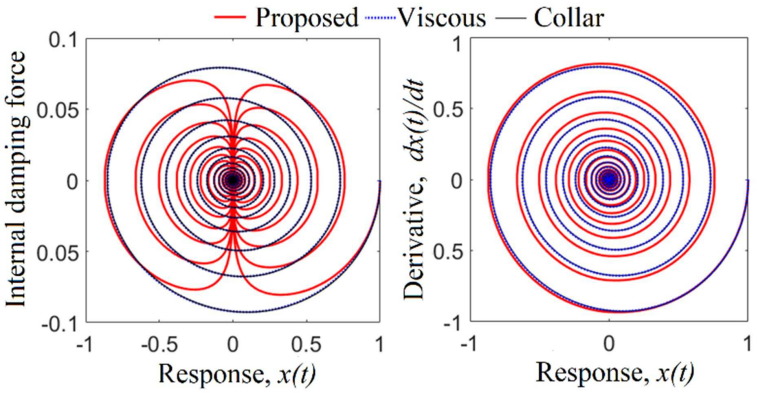

FIG. 11. a) Internal damping force and b) phase-plane plot for free vibration, $\omega_n = 1$, $g = 0.1$.

match between the two is evident. In the proposed approach, there appears to be artefacts ("kinks") in the damping force. These "kinks", which are purely numerical in nature, do not have an effect on the response.

In Fig. 12, we compare the response and hysteresis loops of our proposed model to the viscous and Reid's models for the case of harmonic forced vibration

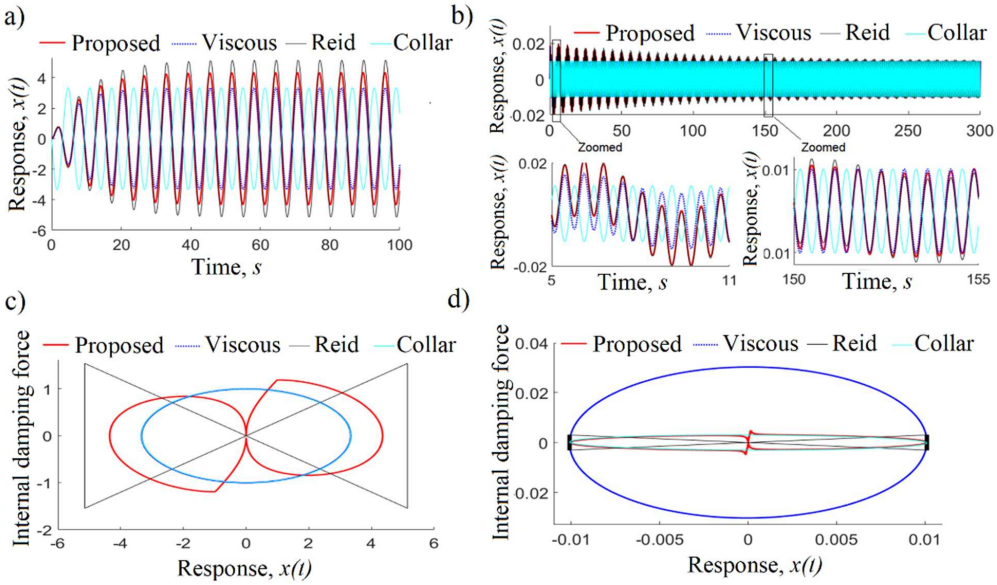

FIG. 12. Comparing responses and hysteresis loops from our proposed model to those from viscous, Reid and Collar models at different excitation frequencies; a), c) $\omega_0 = \omega_n$, b), d) $\omega_0 = 10\omega_n$ for harmonic forced vibration, $\omega_n = 1$, $g = 0.3$. Collar's solution is the steady-state solution.

with different excitation frequencies. The results show that our model is closer in predictions to the viscous model, and that Reid's model overestimates the response. Also, the match between Collar's steady-state solution and the viscous model is evident, and this is not surprising because Collar's solution utilizes the frequency of motion as an inverse proportionality to the damping coefficient. The results also show how the area of the hysteresis loop scales up with the increase of frequency for the viscous model as compared to the others.

In Fig. 13 we show the calculated loss factor g from the three models; viscous, Reid and proposed models for different value of g. The loss factor is calculated from the models as the dissipated energy per cycle divided by the maximum elastic energy at that cycle computed at the steady state (after long t), i.e.:

$$\text{loss factor} \equiv \frac{\oint F_D \, \mathrm{d}x}{2\pi \frac{1}{2} k x_{\max}^2} \tag{5.2}$$

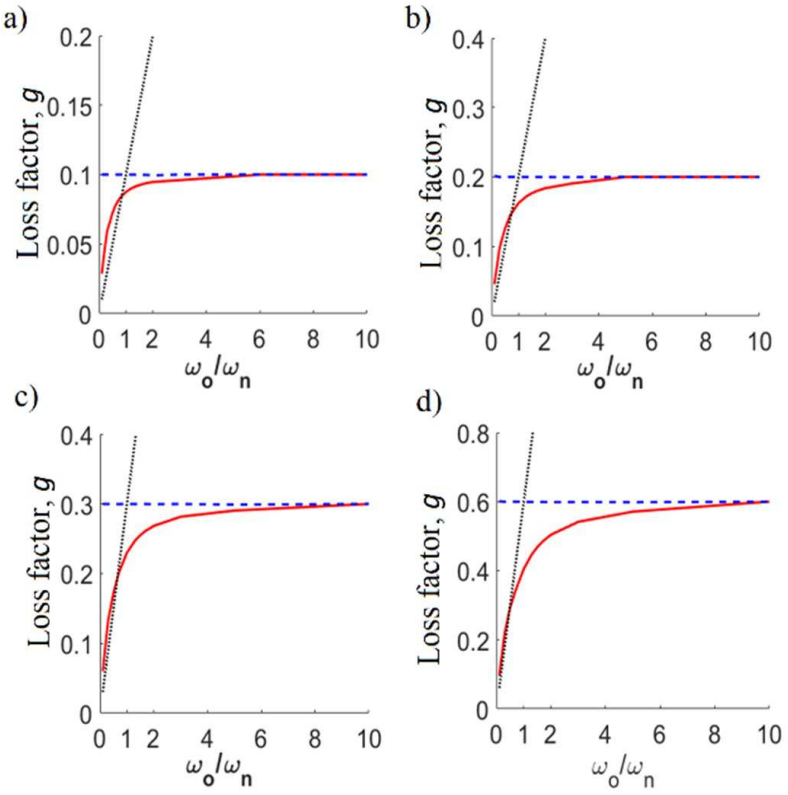

FIG. 13. Comparison between the proposed, Reid, and viscous models for calculation of loss factor under simple sinusoidal excitation for a) $g = 0.1$, b) $g = 0.2$, c) $g = 0.3$, and d) $g = 0.6$. Red solid, black dotted, and blue dashed lines correspond to the proposed, viscous and Reid models, respectively.

where $\oint F_D \mathrm{d}x$ is the energy dissipated per one cycle at steady-state. The loss factor is considered a universal measure for damping in materials and structures [40] and is generally obtained for a material experimentally. Figure 14 shows that the Reid model predicts a constant loss factor while the viscous model produces a loss factor that rises linearly as a function of frequency. Our proposed model produces an interesting prediction of the loss factor. For $\omega_0 < \omega_n$ the proposed model is closer in behavior to the viscous model, and as $\omega_0 > \omega_n$ it becomes asymptotically similar to Reid's model, where it becomes independent of the driving frequency. This trend is consistent with many experimental observations where the damping or loss factors have a weak dependency on frequency. It slightly increases from a non-zero value for low frequencies until it peaks around the resonance frequency then remains nearly constant and decreases at a very slow rate as the frequency increases. The proposed model does capture this trend unlike the Reid model which produces strictly constant damping at any input frequency. Field measurements [41] on actual framed buildings show this kind of trend, where the authors concluded that a new measure for damping must be established because the values of damping depend on the method of measurement. The trend was clearly observed in measuring the loss factor [42] on tempered and laminated glass plates. Also, the same trend was observed in testing damping of metal composite plates by [43]. Other experiments [44] on free vibration of suspended steel box beam showed that a loss factor does remain nearly constant with a slight decrease by increasing frequency far beyond first resonance.

In Fig. 14 we compare the internal damping force from our proposed solution to that from Reid's frictional hysteresis model [12, 27]. As can be seen, Reid's

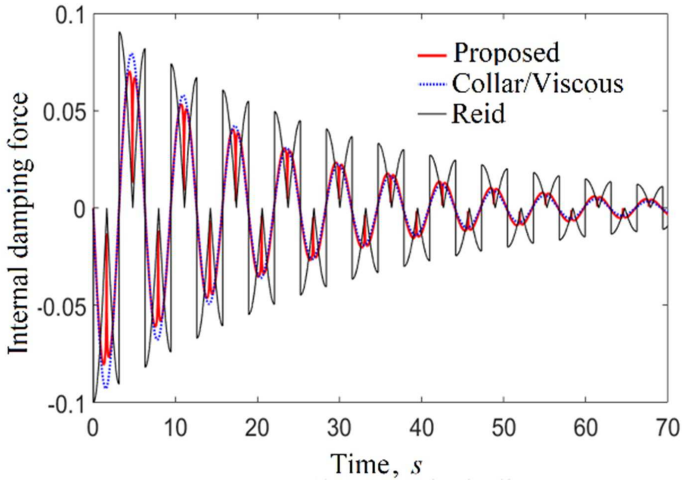

Fig. 14. Comparing the internal damping forces for Collar, Reid and proposed solutions. Free vibration case with $w_n = 1$; $g = 0.1$.

model suffers bigger disadvantage due to such numerical artefacts compared to our model. Our proposed solution remains more faithful to the original Collar's solution.

In Figs. 14 and 15 we compare results of internal damping force as predicted by Reid, viscous, Collar and our proposed model for free and forced vibration. The Reid model [12, 27] is based on the linear Columb friction model which assumes that the damping force is in phase with velocity but depends on the displacement rather than the velocity. The internal damping force as proposed by the Reid model is written as:

$$F_D = kg|x|\frac{\dot{x}}{|\dot{x}|}. \tag{5.3}$$

The dependence on displacement is necessary to produce a frequency-independent energy loss, while the direction of force is maintained to coincide with that of a viscous model. This produces discontinuity in the damping force whenever the velocity changes sign. This discontinuity in the Reid model is evident in Fig. 14 where there is a sudden change in the direction of the damping force. The proposed model compares quite well with both Collar's and viscous solutions, with the "kinks" in the proposed model being the only distinguishing feature between them. The Reid model seems to produce higher values of damping force compared to the other models. It is noted that these kinks have no effect on the smoothness of the response or its derivatives as evidently seen in the figures, particularly Fig. 11 which compares two diagrams: damping force vs. displacement (xF_D), and velocity vs displacement ($x\dot{x}$).

Figure 15 compares the resulting hysteresis loops from the proposed model against viscous and Reid models for a SDOF with different harmonic excitations

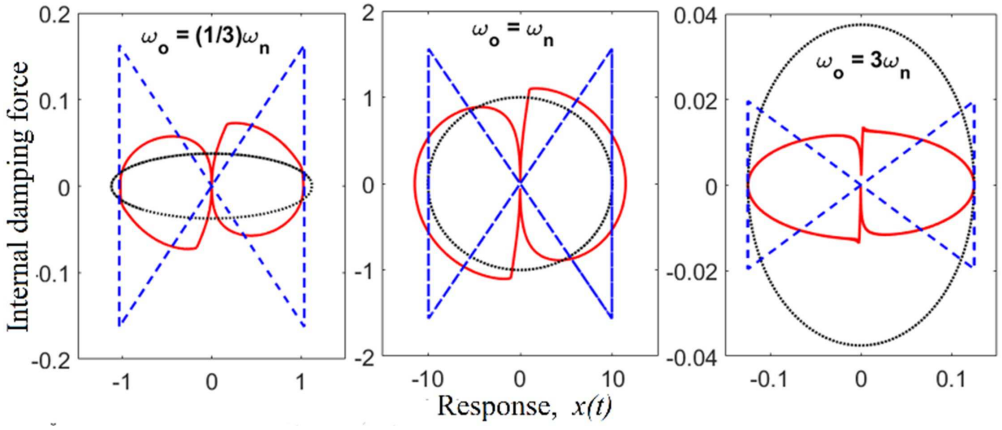

FIG. 15. Comparing steady hysteresis loops of the 3 models for different levels of excitation frequencies for $g = 0.1$. Red solid line = Proposed model, Blue dashed line = Reid model, and Black dotted line = Viscous model.

$= \sin(\omega_0 t)$. When $\omega_0 = \omega_n$ the proposed model and the viscous models are similar in shape with slight variation in the area of the loop. The Reid model produces larger amplitudes of damping forces. When $\omega_0 > \omega_n$, as seen in Fig. 3, the viscous model produces larger hysteresis loops, indicating larger dissipation of energy. The hysteresis loops from the proposed model and Reid are distinct in shape but are similar in terms of area of the loop, indicating equal energy dissipation. When $\omega_0 < \omega_n$, both Reid and proposed models produce hysteresis loops larger in size as compared to the viscous model.

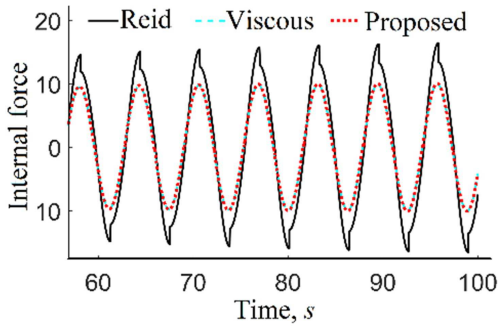

Fig. 16. Comparing total internal force from Reid, viscous and proposed models for the case of harmonic forced vibration at resonance, $w_n = 1$; $g = 0.1$.

Figure 16 shows the total internal force (sum of damping and elastic forces) for the viscous, Reid and proposed models in the steady-state of forced vibration at resonance. The proposed and viscous models match, while the Reid model produces larger amplitudes and discontinuous as seen in the figure.

6. Response to step load

The differences between viscous and hysteretic damping become noticeable in case the excitation is non-harmonic. Particularly, when the excitation force is a constant force applied at $t = 0$, with all-zero initial conditions (step load), the behaviour of hysteretic damper becomes distinguishable from that of viscous damper. Here we compare the results of three models in Fig. 17, namely our proposed model, viscous and Reid–Coulomb friction models. Even for small value of the loss factor ($g = 0.01$) the difference is evident between viscous damping (with damping ratio $\xi = g/2$) and the hysteretic models. The proposed approach is closer to the Reid model, which is considered to be a benchmark model for the case of hysteresis analysis. The Reid model produces relatively larger amplitudes, however the frequencies from all models are almost identical. The difference is amplified in case of stiffer systems as seen in Fig. 17b and c.

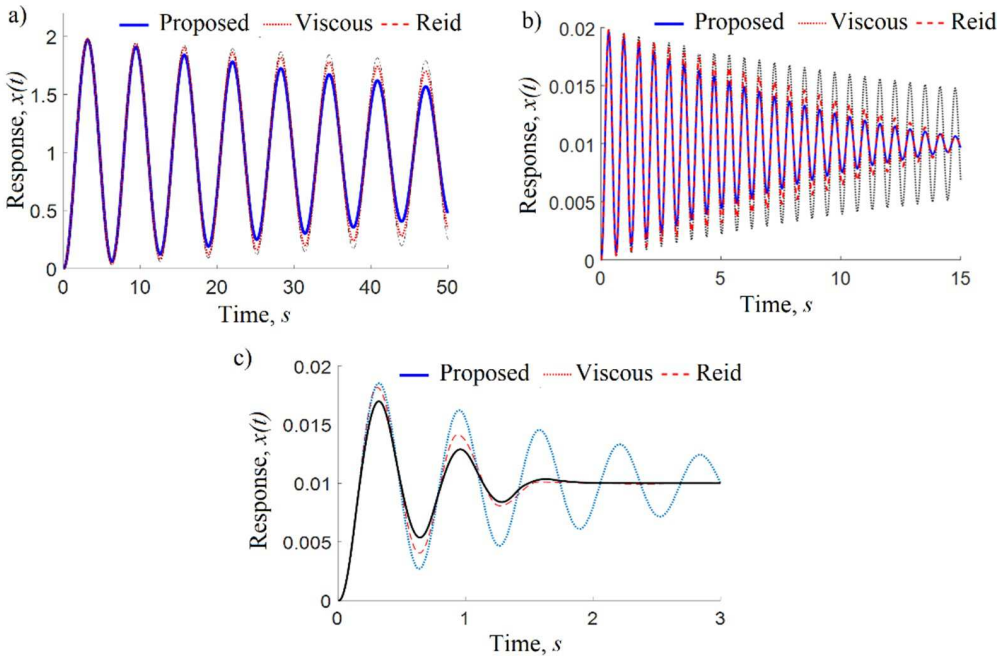

FIG. 17. Comparing the response to a unit constant force using different models, a) $\omega_m = 1$, $m = 1$, $g = 0.01$, b) $\omega_n = 10$, $m = 1$, $g = 0.01$, and c) $\omega_n = 10$, $m = 1$, $g = 0.1$.

From Fig. 17, we see that if we fix the damping ratio in all models (g for hysteresis and $\xi = g/2$ for the viscous), the viscous model produces higher amplitudes for higher stiffer systems (higher natural frequency) because the frequency of motion is a proportionality factor in the viscously dissipated energy. Thus maintaining constant the damping ratio for the viscous system does not cause the dissipated energy to be constant. This is a prime distinction between the viscous and hysteretic models in general. Thus having higher natural frequency in the viscous model (with fixed damping ratio) means higher dissipated energy and this means higher amplitudes (as the elastic energy is force times amplitude).

7. Linearity of the proposed approach

7.1. Non-linearity of the damping force

It is clear that the proposed model is non-linear, as a direct result of the definition of the instantaneous correction factor $\omega_{\text{ins}} = \sqrt{|\ddot{x}/x|}$ producing a non-constant damping coefficient for the differential equation of motion:

$$m\ddot{x} + g\frac{k}{\omega_{\text{ins}}}\dot{x} + kx = F. \tag{7.1}$$

To further investigate this matter, suppose two responses x_1 and x_2 of the same system and initial value problem for two different excitation functions F_1 and F_2 where at any one given instant t for x_1 the correction factor is $\omega_{\text{ins},1} = \sqrt{|\ddot{x}_1/x_1|}$ and for x_2 it is $\omega_{\text{ins},2} = \sqrt{|\ddot{x}_2/x_2|}$. The response x of the same system to a linear superposition of the excitations $aF_1 + bF_2$, where ab are any two real numbers, would at the same given instant be characterised by a correction factor $\omega_{\text{ins}} = \sqrt{|\ddot{x}/x|}$. In order for this response x to be identical to the linear superposition of the responses $ax_1 + bx_2$, it would need to satisfy the relationship:

$$m\ddot{x} + g\frac{k}{\omega_{\text{ins}}}\dot{x} + kx = a\left(m\ddot{x}_1 + g\frac{k}{\omega_{\text{ins},1}}\dot{x}_1 + kx_1\right) + b\left(m\ddot{x}_2 + g\frac{k}{\omega_{\text{ins},2}}\dot{x}_2 + kx_2\right) \tag{7.2}$$

which, by replacing $x = ax_1 + bx_2$, yields:

$$\frac{a\dot{x}_1 + b\dot{x}_2}{\omega_{\text{ins}}} = \frac{a\dot{x}_1}{\omega_{\text{ins},1}} + \frac{b\dot{x}_2}{\omega_{\text{ins},2}}. \tag{7.3}$$

Replacing the correction factors as per Eq. (3.3) and after some manipulations we obtain:

$$(a\dot{x}_1 + b\dot{x}_2)\sqrt{\left|\frac{ax_1 + bx_2}{a\ddot{x}_1 + b\ddot{x}_2}\right|} = a\dot{x}_1\sqrt{\left|\frac{x_1}{\ddot{x}_1}\right|} + b\dot{x}_2\sqrt{\left|\frac{x_2}{\ddot{x}_2}\right|}. \tag{7.4}$$

Generally, it cannot be expected that Eq. (7.4) will be true at every instant and for any set of responses x_1 and x_2, except in the case that both x_1 and x_2 are harmonic functions having the same frequency, thus proving the ex principio non-linearity of the model.

7.2. Near-linearity of the overall system response

At the same time, we have confirmed for various excitations, including harmonic and non-harmonic periodic signals, that the dynamical model for the complete system, although its damping term is non-linear still produces the approximately linear behaviour that is expected of dynamical systems with linear stiffness. Figure 18 demonstrates this in a straightforward manner, whereby the superposition of the obtained responses x_1 and x_2 of the same system for two different simple harmonic excitation functions F_1 and F_2 is nearly (but not exactly) identical to the response x of the system to the superposition of the excitations $F_1 + F_2$. This is a characteristic of not only the presented model, but also of a number of other models with non-linear damping and linear stiffness, such as Reid's model, particularly in cases where the damping forces are low in comparison to the elastic restoring forces.

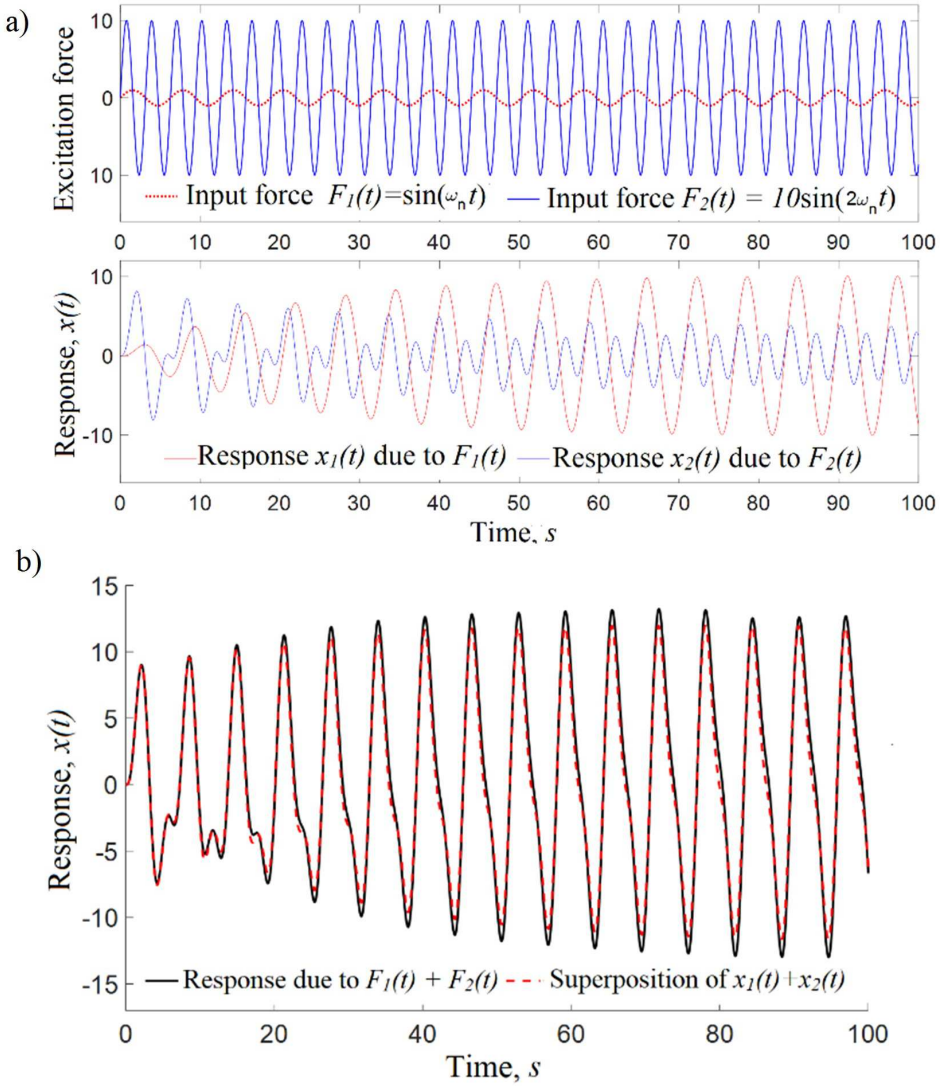

FIG. 18. Comparing the superposition of the responses due to and against the response to the combined forces. a) Input forces and the corresponding responses. b) Response due to the sum of forces compared to linear superposition.

7.3. Linearity within each numerical solution step

Although Eq. (7.1) is globally non-linear, as shown in Section 7.1, we nonetheless note that in in the context of each time step during its numerical integration, ω_{ins} is instantaneously computed and stays as constant within the same time step, as per Fig. 1. Thus Eq. (7.1) is instantaneously treated as a linear differential equation with constant coefficients and the merits of linear modal

superposition are valid within each iteration. In fact, if a general solution can be written in terms of the variable correction factor within the whole time increment, it will depend only on the initial state of the time increment in particular. Thus, that solution can be used to generate the recursive relation for the corrective factor ω_{ins}.

It is worth mentioning here that the proposed procedure maintains the causality principle. This is because the proposed method simply solves classically viscously damped system (which is inherently causal) but with the damping coefficient updated at each time increment.

8. Conclusions

In this article, the hysteretic damping is reproduced in the time-domain with an elegant and simple mathematical formulation that requires no prior knowledge of an excitation frequency or eigenfrequency and adapts autonomously to varying conditions. Also, the model does not need the entire history of motion as it is the case with the models that utilize the Hilbert transforms or quasi-hysteretic models.

The proposed hysteretic damping model is derived through a significant modification to the viscous damping model and utilizes local updating of the damping force through the instantaneous correction factor ω_{inst}. The model bears physical meaning and does not rely on internal state variables.

Overall, the proposed method produces results that are quite similar to the others. Generally, all models agree with each other for a small value of loss factor. The higher the loss factor, the more evident the differences that appear. Thus a final judgement would be left to precise experiments – which are as yet unavailable – to decide on which one is the most accurate. However, the proposed approach has the privilege of simplicity and generalisability over the other solutions for any kind of loading scenario, not only harmonic, as was demonstrated with a step loading scenario.

The mathematical description of the model requires further enhancement in order to get rid of the artefacts that occur for oscillating ω_{ins} (at $x_i = 0$) if the recurrence procedure is used. The model holds promising versatility for expanding into structures with multiple degrees of freedom and hence for modelling elastodynamics of continuum materials with hysteretic internal damping, and these will be the topics of future studies.

Acknowledgements

The authors kindly acknowledge the financial support from the grants "Nonlinear hysteretic damping of graded nanocomposite honeycomb structures for

vibration-optimised design of artificial space satellites (HYST)" (Nazarbayev University, SOE2017005) and "Vibration- and weight-optimised shape memory metal-matrix-composite honeycomb architecture for satellite structures (VSAT)" (Ministry of Education and Science, Kazakhstan, AP05134246).

References

1. M.J. PRIESTLEY, D.N. GRANT, *Viscous damping in seismic design and analysis*, Journal of Earthquake Engineering, **9**, 2, 229–255, 2005.
2. J.M. KELLY, *The role of damping in seismic isolation*, Earthquake Engineering & Structural Dynamics, **28**, 1, 3–20, 1999.
3. E. SOROKIN, *On Theory of Internal Damping in Elastic System Vibration*, Gosstroiizdat, Moscow, 1960.
4. A.L. KIMBALL, D.E. LOVELL, *Internal friction in solids*, Physical Review, **30**, 6, 948, 1927.
5. R.E.D. BISHOP, *The treatment of damping forces in vibration theory*, The Aeronautical Journal, **59**, 539, 738–42, 1955.
6. S. NEUMARK, *Concept of complex Stiffness Applied to Problems of Oscillation with Viscous and Hysteretic Damping*, Aero Research Council R&M, London, 1962.
7. R.E.D. BISHOP, *The general theory of hysteretic damping,* The Aeronautical Quarterly, **7**, 1, 60–70, 1956.
8. R.E.D. BISHOP, D.C. JOHNSON, *The Mechanics of Vibration*, Cambridge University Press, Cambridge, 2011.
9. T.K. CAUGHEY, *Vibration of dynamic system with linear hysteretic damping (linear theory)*, Proceedings of 4th US National Congress of Applied Mechanics – ASCE, **1**, 87–97, 1962.
10. S.H. CRANDALL, *The role of damping in vibration theory*, Journal of Sound and Vibration, **11**, 1, 3–18, 1970.
11. N.O. MYKLESTAD, *The concept of complex damping,* Journal of Applied Mechanics-Transactions of the ASME, **19**, 3, 284–6, 1952.
12. T.J. REID, *Free vibration and hysteretic damping*, The Aeronautical Journal, **60**, 544, 283, 1956.
13. S.H. CRANDALL, *The hysteretic damping model in vibration theory*, Proceedings of the Institution of Mechanical Engineers, Part C: Mechanical Engineering Science, **205**, 1, 23–28, 1991.
14. N. MAKRIS, *Causal hysteretic element,* Journal of Engineering Mechanics, **123**, 11, 1209–1214, 1997.
15. G.B. MURAVSKII, *Linear models with nearly frequency independent complex stiffness leading to causal behaviour in time domain*, Earthquake Engineering & Structural Dynamics, **36**, 1, 13–33, 2007.

16. A.M. Ribeiro, N. Maia, J.M. Silva, *Free and forced vibrations with viscous and hysteretic damping: a different perspective*, Proceedings MZD-5th International Conference of Mechanics & Materials in Design, 2006.

17. N. Nakamura, *Practical causal hysteretic damping*, Earthquake Engineering & Structural Dynamics, **36**, 5, 597–617, 2007.

18. J.A. Inaudi, J.M. Kelly, *Linear hysteretic damping and the Hilbert transform*, Journal of Engineering Mechanics, **121**, 5, 626–632, 1995.

19. S. Adhikari, *Dynamics of nonviscously damped linear systems,* Journal of Engineering Mechanics, **128**, 3, 328–339, 2002.

20. J.A. Inaudi, N. Makris, *Time-domain analysis of linear hysteretic damping*, Earthquake Engineering & Structural Dynamics, **25**, 6, 529–545, 1996.

21. A. Reggio, M. De Angelis, *Modelling and identification of structures with rate-independent linear damping,* Meccanica, **50**, 3, 617–632, 2015.

22. R.H. Scanlan, *Linear damping models and causality in vibrations*, Journal of Sound and Vibration, **13**, 4, 499–503, 1970.

23. Y.I. Bobrovnitskii, *Hysteretic damping and causality*, Acoustical Physics, **59**, 3, 253–256, 2013.

24. R. Bouc, *Forced vibrations of mechanical systems with hysteresis*, Proceedings of the Fourth Conference on Nonlinear Oscillations, Prague, 1967.

25. Y.K. Wen, *Method for random vibration of hysteretic systems*, Journal of the Engineering Mechanics Division, **102**, 2, 249–263, 1976.

26. F. Ikhouane, V. Mañosa, J. Rodellar, *Dynamic properties of the hysteretic Bouc–Wen model*, Systems & Control Letters, **56**, 3, 197–205, 2007.

27. G.B. Muravskii, *On frequency independent damping*, Journal of Sound and Vibration, **274**, 3-5, 653–668, 2004.

28. C. Spitas, *A continuous piecewise internal friction model of hysteresis for use in dynamical simulations*, Journal of Sound and Vibration, **324**, 1-2, 297–316, 2009.

29. H.G. Küssner, *Schwingungen von flugzeugflügeln*, Jahrbuch der Deutscher Versuchsanstalt für Luftfahrt, Section E3 Einfluss der Baustoff-Dämpfung, 319–20, 1929.

30. H.G. Küssner, *Augenblicklicher Entwicklungsstand der Frage des Flugelflatterns*, Luftfahrtforschung, **12**, 193, 1935.

31. R. Kassner, *Die Berucksichtigung der inneren Dampfung beim ebenen Problem der Flugelschwingung*, Luftfahrtforsch, **13**, 11, 388–393, 1936.

32. R.E.D. Bishop, W.G. Price, *A note on hysteretic damping of transient motions*, Studies in Applied Mechanics, **14**, 39–45, 1986.

33. N. Maia, *Reflections on the hysteretic damping model*, Shock and Vibration, **16**, 5, 529–542, 2009.

34. N.M. Maia, J.M. Silva, A.M. Ribeiro, *On a general model for damping*, Journal of Sound and Vibration, **218**, 5, 749–767, 1998.

35. M. Horodinca, *Experimental investigation of free response on a cantilever beam (first flexural vibration mode)*, Bulletin of the Polytechnic Institute of Jassy, **6**, 66, 23–34, 2016.

36. M. HORODINCA, N.E. SEGHEDIN, E. CARATA, M. BOCA, C. FILIPOAIA, D. CHITARIU, *Dynamic characterization of a piezoelectric actuated cantilever beam using energetic parameters*, Mechanics of Advanced Materials and Structures, **21**, 2, 154–164, 2014.

37. L.Y. CHEN, J.T. CHEN, C.H. CHEN, H.K. HONG, *Free vibration of a SDOF system with hysteretic damping*, Mechanics Research Communications, **21**, 6, 599–604, 1994.

38. A.M. RIBEIRO, N.M. MAIA, J.M. SILVA, M. FREITAS, L. REIS, *Free vibration response using the constant hysteretic damping model*, Proceedings of the 11th International Conference on Vibration Engineering, Timisoara, Romania, 65–70, 2005.

39. A.M. RIBEIRO, N.M. MAIA, J.M. SILVA, *On the modelling of damping in structural vibrations*, Proceedings of the International Conference of Noise and Vibration Engineering (ISMA2006), Leuven, Belgium 2006.

40. M. CARFAGNI, E. LENZI, M. PIERINI, *The loss factor as a measure of mechanical damping*, SPIE Proceedings Series, 580–584, 1998.

41. N. FUKUWA, R. NISHIZAKA, S. YAGI, K. TANAKA, Y. TAMURA, *Field measurement of damping and natural frequency of an actual steel-framed building over a wide range of amplitudes*, Journal of Wind Engineering and Industrial Aerodynamics, **59**, 2-3, 325–347, 1996.

42. B. BLOSS, M.D. RAO, *Measurement of damping in structures by the power input method*, Experimental Techniques, **26**, 3, 30–2, 2002.

43. G. PARFITT, D. LAMBETH, *The Damping of Structural Vibrations*, Imperial College, London, 1960.

44. J.G. MCDANIEL, P. DUPONT, L. SALVINO, *A wave approach to estimating frequency-dependent damping under transient loading*, Journal of Sound and Vibration, **231**, 2, 433–449, 2002.

Received April 11, 2020; revised version June 15, 2020.
Published online August 10, 2020.